Comparison of Discrete-Laser and Comb-Based DWDM Analog Coherent Links in the Presence of Fiber Kerr Nonlinearity

Elizabeth Chen and Joseph M. Kahn

***Abstract*—We study O-band dense wavelength-division multiplexed (DWDM) analog coherent systems that use either discrete lasers or electro-optic frequency comb generators as transmitter and local oscillator (LO) light sources, considering the effects of fiber Kerr nonlinearity. We study the performance of links using 17 channels at 56 GBaud with 100-GHz spacing, comparing three dual-polarization modulation formats: quadrature phase-shift keying (QPSK), 8-ary phase-shift keying (8-PSK) and 16-ary quadrature amplitude modulation (16-QAM), which achieve aggregate bit rates of 3.4 Tb/s, 5.1 Tb/s and 6.8 Tb/s, respectively, after accounting for forward error-correction overhead. We find that comb systems suffer a 2-dB degradation in signal-to-noise ratio compared to discrete-laser systems from comb processing losses and booster amplification noise, but can still support more than 10 km of transmission distance with unallocated loss margins of more than 10 dB for QPSK, 7 dB for 8-PSK, and 2 dB for 16-QAM. We find that the achievable transmission distance can depend on timing skew between different channels because of both linear and nonlinear crosstalk. While QPSK comb systems are insensitive to timing skew, 8-PSK and 16-QAM comb systems tolerate maximum timing skews of 0.2 times and 0.1 times the symbol period, respectively, with less than a 1-km penalty on achievable transmission distance.**

***Index Terms*—Coherent detection, data centers, optical frequency comb, fiber nonlinearity, O-band, dense wavelength-division multiplexing.**

I. Introduction

To accommodate the rapid growth of Internet traffic, optical interconnects in data centers must continue scaling in bandwidth and spectral efficiency [1]. Coherent transceivers are attractive [2], because they allow data to be encoded onto all degrees of freedom in the signal field, enabling the use of advanced modulation formats that increase spectral efficiency [3]. In addition, coherent receivers mix received signals with a strong local oscillator (LO), yielding improvements in receiver sensitivity and link budget that help support advanced network architectures and highly integrated subsystems [4].

To avoid the potentially power-hungry high-speed digital signal processing (DSP) operations found in traditional long-haul coherent links, power-efficient analog coherent data center link architectures have been proposed [5], [6]. Analog coherent link architectures save power by performing polarization control and carrier recovery using optics and analog electronics, possibly augmented by low-speed DSP. Eliminating DSP-based dispersion compensation is enabled by operating in the O-band, where chromatic dispersion is low.

Although operation near the zero-dispersion wavelength in the O-band obviates the need for dispersion compensation, it can exacerbate fiber Kerr nonlinear effects [7], which include self-phase modulation (SPM), cross-phase modulation (XPM), and four-wave mixing (FWM). For example, O-band wavelength-division multiplexed (WDM) links using intensity modulation and direct detection (IM/DD) are limited by FWM [8]. FWM effects are enhanced in these IM links because of the strong carrier component present in IM signals [9], [10].

While dense WDM (DWDM) analog coherent links in the O-band benefit from using suppressed-carrier modulation formats, they are not able to exploit some Kerr nonlinearity-mitigating factors present in traditional C-band DWDM coherent systems. For example, in contemporary dispersion-unmanaged C-band DWDM coherent systems, XPM effects are reduced by pulse walk-off [11] and FWM effects are suppressed because dispersion destroys the phase matching between different channels [12]. These systems rely on DSP-based dispersion compensation and nonlinear compensation methods. Similarly, in legacy dispersion-managed C-band DWDM coherent systems, Kerr nonlinearity impairments are mitigated by leaving residual dispersion at the end of each span to break phase matching for FWM [13], while XPM effects can be reduced by engineering the link dispersion profile [14] or introducing time skews between the signal waveforms of different channels [15].

O-band DWDM analog coherent systems, in contrast, cannot exploit fiber dispersion to substantially mitigate Kerr nonlinear effects. Likewise, these systems cannot rely on erbium-doped fiber amplifiers to boost signal power. Managing loss and maintaining sufficient signal-to-noise ratio (SNR) therefore become critical design considerations for O-band analog coherent systems in data centers, where ample link budget is required [1].

Frequency combs are increasingly attractive candidates for light sources in WDM data center systems [16]. Comb sources obviate the need for multiple discrete lasers, which can save power needed for laser thermal stabilization [17]. In addition, the phase coherence of comb lines offers opportunities to perform joint phase recovery and reduce complexity at the receiver [18], [19]. Dispersion-unmanaged DWDM coherent transmission in the C-band using comb sources has been demonstrated [20], and is found to outperform transmission using discrete laser sources, as the frequency stability of comb lines maximizes the effectiveness of digital backpropagation for compensating fiber dispersion and Kerr nonlinearity [21]. O-band comb-based coherent transmission using DSP-based transmitter (Tx) and receiver (Rx) signal processing has also

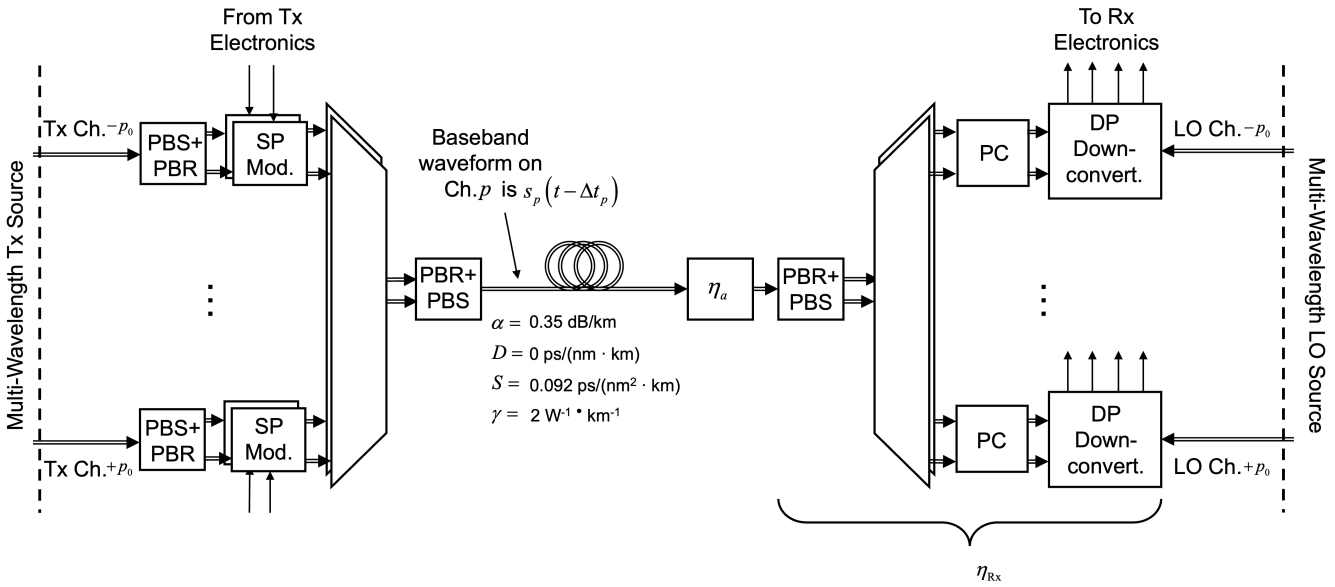

Fig. 1. O-band analog coherent link model. The multi-wavelength source for both the transmitter (Tx) and the local oscillator (LO) can be either a bank of discrete lasers or a frequency comb generator. At the fiber input, the baseband signal waveform on channel p has the form $s_p\,(t-\Delta t_p)$, where Δt_p models timing skew. η_{Rx} denotes the total loss between the input of the polarization beam rotator and splitter (PBR + PBS) and the input of the dual-polarization (DP) downconverter. η_a is an additional loss incurred at the end of the fiber to quantify loss margin. Ch.: channel, SP: single-polarization, mod.: modulator, PC: polarization controller, downconvert.: downconverter, and Rx: receiver.

been experimentally demonstrated [22].

While O-band DWDM analog coherent links using either discrete lasers [23] or frequency combs [24], [19] as multi-wavelength sources have been studied, to our knowledge, no published works have quantified and compared their performance in the presence of fiber Kerr nonlinearity. Such a comparison is the subject of this paper. We find that even when using efficient electro-optic comb generators [25] as Tx and LO sources, the need to de-interleave, flatten, amplify and demultiplex the Tx and LO combs decreases the link SNR by about 2 dB compared to discrete-laser links, decreasing the achievable transmission distance by about 5 km. In both comb-based and discrete-laser links, Kerr nonlinearity reduces achievable transmission distances compared to dispersion-limited distances. It also causes nonlinear crosstalk, making the link more sensitive to timing skew, especially for higher-order modulation formats.

The remainder of this paper is organized as follows. Section II describes the system model used for this work. Section III discusses the effects of loss and additive noise on O-band analog coherent links that use either combs or discrete lasers as light sources. Section IV discusses the effects of timing skew between channels. Section V concludes the paper.

II. System Model

We model the multi-channel O-band analog coherent link as shown in Fig. 1. The channels are indexed by an integer p, where $-p_0 \le p \le +p_0$, and are separated by frequency f_m. In this section, we describe key subsystems of the system model.

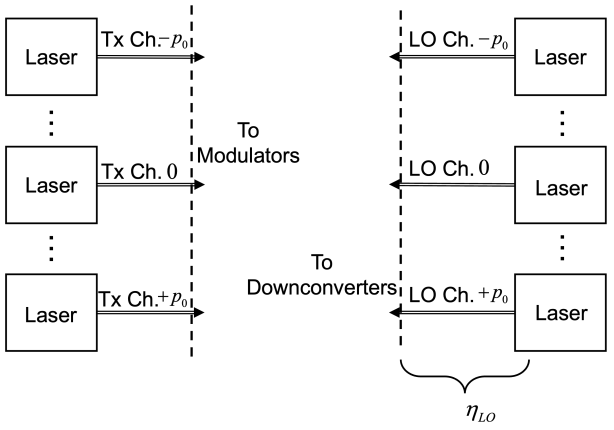

Fig. 2. Banks of discrete lasers as the Tx and LO multi-wavelength sources. η_{LO} denotes the LO path loss between the laser output and DP downconverter in Fig. 1.

A. Multi-Wavelength Light Source

The multi-wavelength light sources indicated in Fig. 1 can be either banks of discrete lasers or frequency comb generators, as shown in Fig. 2 or Fig. 3, respectively. We consider the dual-resonator electro-optic (DR-EO) frequency comb generator in this study because it has high power conversion efficiency, electronically tunable comb spacing, and well-studied phase noise behavior [24], [26]. These characteristics make the DR-EO frequency comb generator a good candidate for comb-based analog coherent links.

When using a bank of discrete lasers, the laser for channel p will carry a phase noise $\varphi_p\,(t)$, which is modeled by a Wiener process [27]. We show in Appendix A that the coherence time of the phase noise process is much longer than the

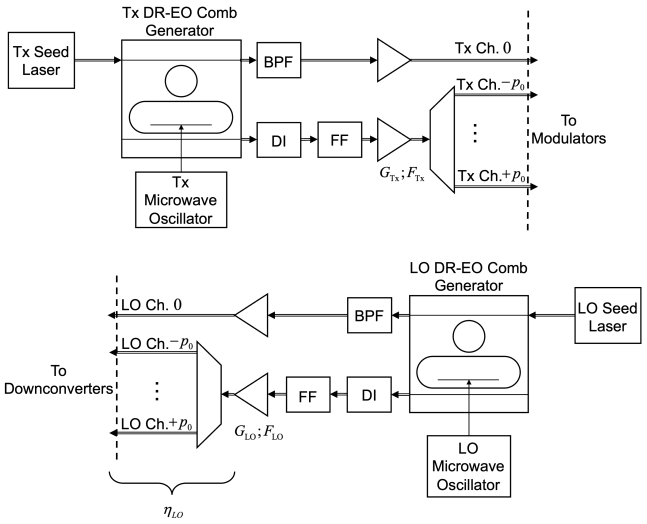

Fig. 3. Dual-resonator electro-optic (DR-EO) frequency comb generators as the Tx and LO multi-wavelength sources. G_{Tx} and F_{Tx} are, respectively, the gain and noise figure of the Tx booster amplifier. G_{LO} and F_{LO} are, respectively, the gain and noise figure of the LO booster amplifier. BPF: bandpass filter, DI: de-interleaver, and FF: flattening filter.

memory length of the fiber dispersion. Thus, in order to isolate the interplay of dispersion and Kerr nonlinear effects in fiber propagation, we can model the laser phase noise on channel p, given by φ_p, as constant in time and independent, identically distributed (i.i.d.) following a uniform distribution, i.e., $\varphi_p \sim U\left[-\pi, \pi\right]$.

When using a DR-EO frequency comb generator, the phase noise on the p-th channel has the form

$$\varphi_p\left(t\right) = \varphi_o\left(t\right) + p\varphi_m\left(t\right), \tag{1}$$

where $\varphi_o\left(t\right)$ is the optical phase noise of the DR-EO comb seed laser and follows a Wiener process, and $\varphi_m\left(t\right)$ is the phase noise of the modulator microwave drive signal [24]. Following an argument similar to that in the discrete-laser case, we model the phase noise on channel p, $\varphi_p = \varphi_o + p\varphi_m$, as constant in time, with $\varphi_o \sim U\left[-\pi, \pi\right]$ and $\varphi_m \sim U\left[-\pi, \pi\right]$.

When using a frequency comb source, the comb lines undergo pre-processing by a de-interleaver (DI), flattening filter (FF), or bandpass filter (BPF) as needed before data modulation (see Fig. 3). Since the frequency comb output power is shared by multiple comb lines, the power on any given comb line is typically lower than that of a single-wavelength laser [28]. Comb-based sources therefore require optical amplification to reach a sufficient signal power [19], [22]. The semiconductor optical amplifiers (SOAs) shown for the Tx and LO comb sources add amplified spontaneous emission (ASE) noise, which is modeled as having a one-sided power spectral density (PSD) of

$$S_{i,boost.}\left(f\right) = \frac{\left(G_i - 1\right)F_i hc}{2\lambda}, \tag{2}$$

where G_i and F_i represent, respectively, the gain and noise figure of either the Tx booster amplifier (G_{Tx} and F_{Tx}) or LO booster amplifier (G_{LO} and F_{LO}). h and c are Planck's constant and the speed of light, respectively.

B. Modulator, (De-)Multiplexer, Fiber, and Additional Attenuation

Each modulator block shown in Fig. 1 modulates the in-phase (I) and quadrature (Q) components of the two polarizations using dual-arm Mach-Zehnder modulators (MZMs). We assume ideal MZM characteristics and model the I and Q components of the modulator output signal in each polarization as a sequence of rectangular pulses filtered by a 5-th order Bessel lowpass filter (LPF).

At the fiber input, the different wavelength channels are multiplexed using an arrayed waveguide grating (AWG). In the model, the baseband frequency response of the AWG for each channel is super-Gaussian [29]. At the fiber output, the different wavelength channels are also demultiplexed using an AWG.

We model signal propagation through fiber using the nonlinear Schrödinger equation (NLSE). The simulation code used implements the NLSE via the split-step Fourier method (SSFM) [30] and includes chromatic dispersion, fiber Kerr nonlinearity, and fiber attenuation. The step size for the SSFM simulation is set to 200 m. For chromatic dispersion, the dispersion parameter D is set to zero while the dispersion slope S is set to 0.092 ps/(nm^2·km) to reflect centering the system at the zero-dispersion wavelength in standard SMF-28 fiber. We neglect birefringence in the fiber since polarization-mode dispersion and other associated effects are weak in short-reach links [31], and we wish to isolate the combined effects of chromatic dispersion, nonlinearity, and loss.

The fiber Kerr nonlinearity strength is described by the nonlinear parameter γ:

$$\gamma = \frac{2\pi\bar{n}_2}{\lambda A_{eff}}. \tag{3}$$

In Eq. (3), $\bar{n}_2$ is the nonlinear refractive index coefficient, which is $\bar{n}_2 \approx 2.6\times10^{-20}$ m^2·W^{-1} for pure silica glass [32]. A_{eff} is the effective mode area. In standard SMF-28 fiber, the mode-field diameter at the zero-dispersion wavelength is 9.2 μm, and the effective mode area can be estimated as $A_{eff} \approx \pi\left(9.2/2\right)^2\,\mu\mathrm{m}^2 \approx 66\ \mu\mathrm{m}^2$. Using Eq. (3), we estimate the nonlinear parameter to be $\gamma \approx 2$ W$^{-1}\cdot$ km^{-1} for O-band transmission.

The overall signal loss between the output of the fiber and the input of the DP downconverter is η_{Rx}, as indicated in Fig. 1. In order to characeterize the loss margin achieved by the system, we insert an additional loss η_a. Since fiber nonlinear effects are more severe at high signal powers, η_a is placed at the end of the fiber to simulate a worst-case loss.

C. Coherent Receiver

At the receiver, the full signal field is recovered using dual-polarization (DP) coherent downconverters, as shown in Fig. 1. In Figs. 2 and 3, the path loss between the output of the LO source and the input of the DP downconverter is η_{LO}. For the frequency comb-based system, η_{LO} includes the insertion loss of the LO comb AWG.

In both the discrete-laser and the comb-based systems, the received electrical signal is further corrupted by additive white

TABLE I
SIMULATION PARAMETERS

Operating wavelength (λ)	1310 nm
Number of channels	17
Baud rate	56 Gbaud
Channel spacing (f_m)	100 GHz
Tx filter bandwidth	42 GHz
Tx SOA gain (G_{Tx})	15 dB
Tx SOA noise figure (F_{Tx})	7 dB
Modulation and multiplexing loss (η_{mod})	-8 dB
Dispersion parameter (D)	0 ps/(nm·km)
Dispersion slope (S)	0.092 ps/(nm^2·km)
Attenuation (α)	0.35 dB/km
Nonlinear parameter (γ)	2 W^{-1}·km^{-1}
SSFM step size	200 m
PBR + PBS, AWG, and PC loss (η_{Rx})	10 dB
Rx AWG super-Gaussian order	1/2
Rx AWG super-Gaussian 3-dB bandwidth	500 GHz
Rx filter bandwidth	30.8 GHz
LO SOA gain (G_{LO})	15 dB
LO SOA noise figure (F_{LO})	7 dB
LO path loss (η_{LO})	0 or -2 dB*
LO power per channel (P_{LO})	12 dBm

* η_{LO} is -2 dB for comb-based systems to reflect the insertion loss of the integrated AWG and 0 dB for discrete lasers-based systems.

Gaussian noise (AWGN) including thermal and shot noise [3]. After downconversion, the signal is filtered by a 5-th order Bessel LPF and undergoes ideal timing recovery and phase offset removal.

Table I summarizes the system simulation parameter values used for the remainder of this paper.

Throughout the paper, we compare the performance of systems that use either DR-EO comb generators or discrete lasers as signal and LO sources. The two system designs are distinguished in simulation as follows. (1) In comb-based systems, owing to the low power of each comb line at the comb generator output, the comb power needs to be boosted by SOAs at both the transmitter and LO (see Fig. 3). Discrete single-wavelength lasers are assumed capable of providing sufficient output power without amplification. Therefore, for the discrete-laser system, $S_{\mathrm{Tx}}(f)$ and $S_{\mathrm{LO}}(f)$ are set to 0. In the comb-based system, $S_{\mathrm{Tx}}(f)$ and $S_{\mathrm{LO}}(f)$ are set according to the parameters in Table I. (2) In the comb-based system, the LO frequency comb must be demultiplexed before being combined with the received signal. The LO path loss, η_{LO}, is set to 2 dB to reflect the insertion loss of the integrated AWG [23].

Several modulation formats are candidates for O-band analog coherent links. In this study, we consider quadrature phase-shift keying (QPSK), 8-ary phase-shift keying (8-PSK), and 16-ary quadrature amplitude modulation (16-QAM). System performance is quantified by the achievable transmission distance, which is the maximum fiber length L over which the WDM signal can be transmitted with equal power per channel while maintaining a pre-forward error correction (FEC) bit-error ratio (BER) not exceeding 2.4×10^{-4} on every channel. This target BER applies to codes such as the RS(544, 514) [33]. The achievable transmission distance is found by plotting the BER for every channel as a function of total launch power at the fiber input. For example, Figs. 4(a)-(b) show that a 16-QAM comb system with an additional link loss of $\eta_a = 2$ dB can achieve a transmission distance of 8.4 km but not 15 km. The total launch power is swept up to 20 dBm to ensure operation below the eye safety limit [34]. If fiber Kerr nonlinearity were neglected, the BERs for all channels would decrease monotonically with increasing launch power.

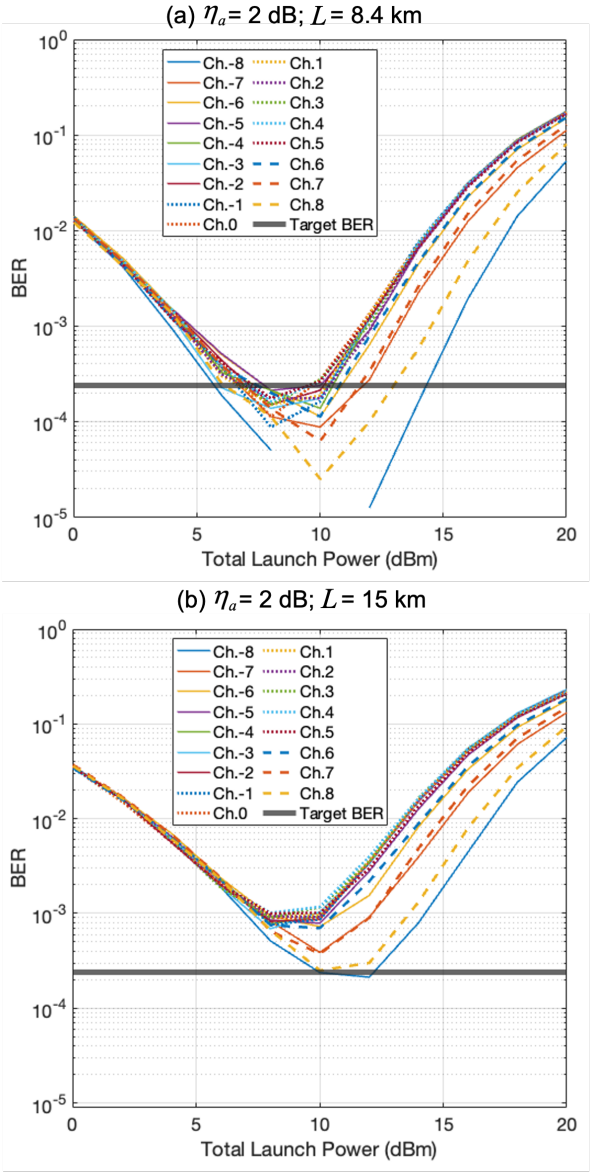

Fig. 4. BER versus total launch power for a 17-channel 16-QAM comb system at transmission distances (a) $L = 8.4$ km and (b) $L = 15$ km with additional link loss $\eta_a = 2$ dB. Assuming a target BER of 2.4×10^{-4}, when the transmission distance is 8.4 km, the total launch power can be optimized to achieve the target BER on every channel. By contrast, when the transmission distance is 15 km, no launch power can achieve the target BER on every channel. Since 8.4 km is the maximum distance over which all channels can achieve the target BER, 8.4 km is the achievable transmission distance of 16-QAM comb systems with additional link loss $\eta_a = 2$ dB.

III. LOSSES AND NOISE

Data center systems benefit from high loss tolerance because it facilitates scaling to higher-order modulation formats, relaxed specifications for existing link components and subsystems, and introduction of new components and subsystems,

This article has been accepted for publication in IEEE/OSA Journal of Lightwave Technology. This is the author's version which has not been fully edited and content may change prior to final publication. Citation information: DOI 10.1109/JLT.2024.3519252

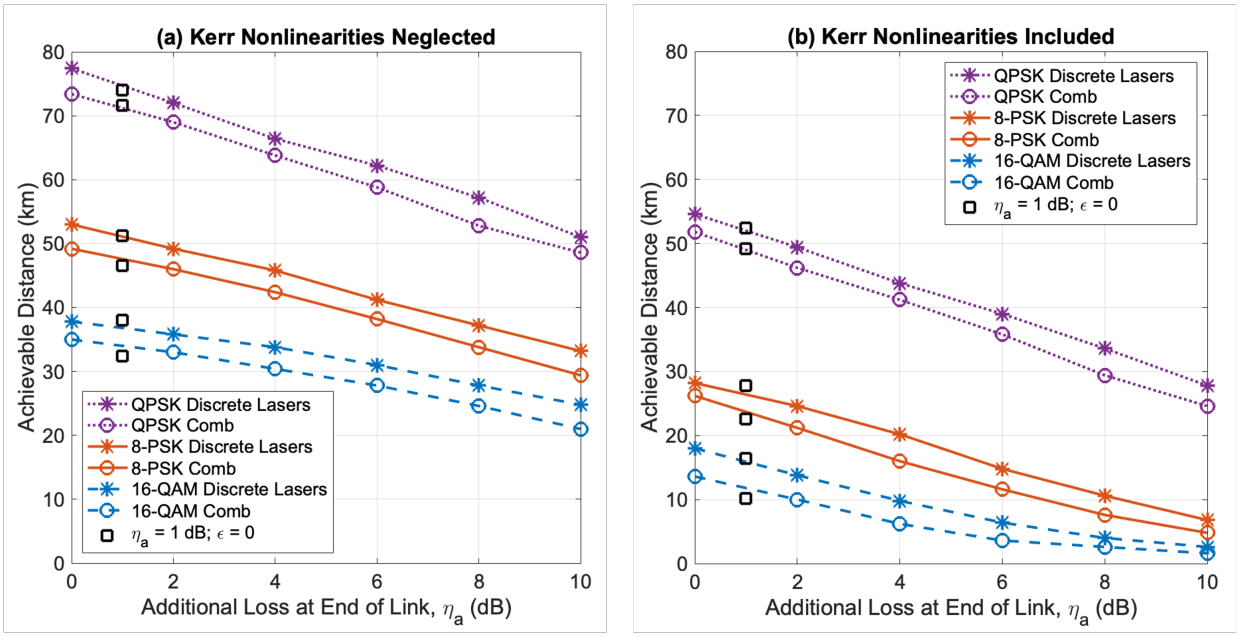

Fig. 5. Achievable distance as a function of the additional loss η_a at the end of the link when fiber Kerr nonlinearity effects are (a) neglected or (b) included. The black squares indicate achievable distances in Fig. 6 at $\eta_a = 1$ dB and peak-to-peak normalized skew $\epsilon = 0$.

For 16-QAM, transmission distances of up to 10 km are supported with additional link losses of 4 dB and 2 dB for discrete-laser and comb-based and systems, respectively. For 8-PSK, transmission distances of up to 10 km are supported with additional losses of 8 dB and 7 dB for discrete laser-based and comb-based systems, respectively. For QPSK, transmission distances of up to 20 km are supported with additional losses exceeding 10 dB for both types of systems.

such as optical switches. In this section, we analyze the effects of losses and noise on O-band analog coherent DWDM systems. We present the achievable transmission distances for systems using QPSK, 8-PSK, or 16-QAM, and discuss differences in loss management requirements between comb-based and discrete laser-based systems.

Figure 5 shows the achievable transmission distance versus additional link loss η_a for the various system designs studied.

When fiber Kerr nonlinearity is neglected (Fig. 5(a)), the difference in achievable transmission distance between discrete laser-based and comb-based systems is about 5 km for QPSK, 8-PSK and 16-QAM for all values of η_a.

When fiber Kerr nonlinearity is included (Fig. 5(b)), achievable transmission distances are reduced substantially. When η_a lies between 0 dB and 5 dB, the difference in achievable transmission distance between discrete laser-based and comb-based systems is also about 5 km for QPSK, 8-PSK and 16-QAM. The ∼5-km reach penalty for low values of additional loss η_a represents an intrinsic penalty from using combs as light sources caused by added losses from comb demultiplexing and flattening, and by added noise from SOAs. The 5-km gap corresponds to an approximate 5 km · 0.35 dB/km ≈ 2 dB penalty in signal-to-noise ratio (SNR) for using combs instead of discrete lasers. Given the power and cost savings offered by comb-based systems, the 2-dB SNR penalty is likely acceptable if the comb-based systems can achieve sufficient transmission distance and loss margin.

Finally, in Fig. 5(b), we observe that when the additional loss η_a lies between 5 dB to 10 dB, the achievable transmission distance curves for 16-QAM comb, 16-QAM discrete-laser, and 8-PSK comb systems begin to flatten, because the short physical fiber length limits the Kerr nonlinearity generation processes.

QPSK systems using discrete lasers or comb sources easily support all intra-data center links and many inter-data center links [35] while offering large loss margins. We see in Fig. 5(b) that when using QPSK, both system designs accommodate transmission links of more than 20 km even when additional link loss is as high as $\eta_a = 10$ dB.

For higher-order modulation formats, constraints on additional link losses need to be tighter, especially when using comb-based sources. For instance, to support all intra-data center links, which have distances $\leq$ 10 km, 8-PSK discrete-laser systems need to have less than 8 dB of additional link losses, while 8-PSK comb systems need to have less than 7 dB of additional link losses. 16-QAM discrete-laser systems need to have less than 4 dB of additional link loss, while 16-QAM comb systems need to have less than 2 dB of additional link loss.

IV. Timing Skew

In this section, we examine the impact of timing skew, which is misalignment between the baseband modulation waveforms of different channels. We observe that skew can affect the impact of linear and nonlinear crosstalk. Linear crosstalk arises on a given channel when neighboring channels leak through the receiver demultiplexer at the fiber output and through the LPF at the downconverter output. Analog DWDM coherent systems, which are not able to take advantage of digital Nyquist pulse shaping, may be more susceptible to

This article has been accepted for publication in IEEE/OSA Journal of Lightwave Technology. This is the author's version which has not been fully edited and content may change prior to final publication. Citation information: DOI 10.1109/JLT.2024.3519252

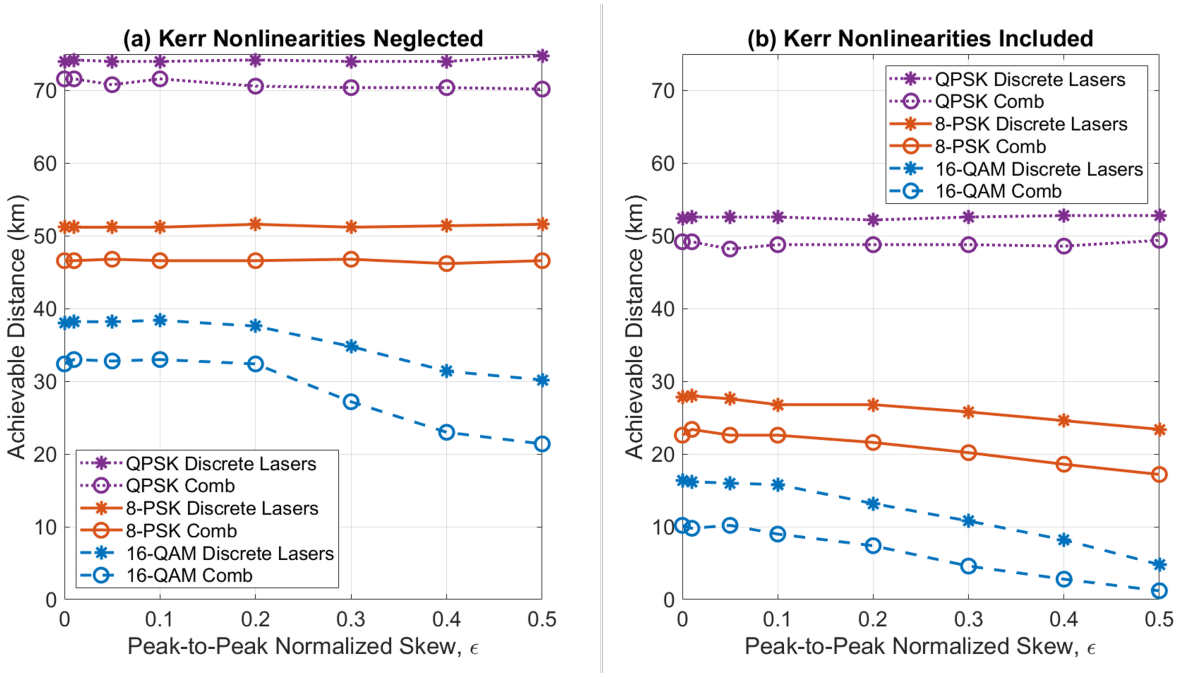

Fig. 6. Achievable transmission distance as a function of peak-to-peak normalized skew, ϵ, when fiber nonlinear effects are (a) neglected or (b) included. The additional link loss is set to $\eta_a = 1$ dB. 16-QAM systems can tolerate peak-to-peak normalized skews of $\epsilon = 0.1$ with less than 1-km penalty in transmission distance. 8-PSK systems can tolerate $\epsilon = 0.2$ with less than 1-km penalty. QPSK systems are not subject to reductions in transmission distance due to skew.

linear crosstalk than their DSP-based counterparts. Nonlinear crosstalk arises on a given channel when it is phase-modulated by neighboring channels by XPM or when its frequency coincides with an interfering component generated by FWM. These nonlinear crosstalk effects are expected to have similar impact in analog or DSP-based DWDM coherent systems, assuming the system designs are otherwise similar.

In our simulations, the skews on different channels are modeled as constant in time and i.i.d. Channel p has a skew Δt_p drawn from a uniform distribution: $\Delta t_p \sim U\left[-\epsilon T_s/2, +\epsilon T_s/2\right]$, where T_s is the symbol period and ϵ is the peak-to-peak skew normalized by the symbol period. Figure 6 shows the achievable transmission distance versus peak-to-peak normalized skew ϵ, for both discrete-laser and comb-based systems using various modulation formats.

Figure 6(a), which neglects fiber Kerr nonlinearity, illustrates the impact of linear crosstalk. The achievable transmission distance is insensitive to skew for QPSK and 8-PSK, and depends significantly on skew for 16-QAM, decreasing noticeably when the skew between any two channels exceeds $0.2T_s$. It is plausible that 16-QAM is most sensitive of the three modulation formats to linear crosstalk because its constellation points have, on average, the largest number of nearest neighbors.

Figure 6(b) includes fiber Kerr nonlinearity, and thus illustrates the impact of both linear and nonlinear crosstalk on achievable transmission distance. The achievable transmission distance remains insensitive to skew for QPSK, while it depends on skew moderately for 8-PSK and strongly for 16-QAM. To avoid a significant decrease in transmission distance, the maximum skew between any two channels should not exceed $0.2T_s$ for 8-PSK and $0.1T_s$ for 16-QAM. For small-to-moderate amounts of skew, $\epsilon \leq 0.3$, the performance gap between discrete-laser and comb-based systems does not widen with increasing skew, suggesting that comb systems are not more severely impacted by timing skew than discrete-laser systems.

The results in Fig. 6(b) suggest that skew management is not critical in QPSK systems and is needed in 8-PSK systems only to achieve transmission distances beyond about 20 km or 15 km in discrete-laser or comb-based systems, respectively. By contrast, in 16-QAM systems, management of skew to a tolerance of about $0.1T_s \approx 2$ ps is likely needed in discrete-laser systems longer than a few km and in all comb-based systems. Skew-management strategies may include controlling the lengths of elecrical traces and optical waveguides, and adjusting the symbol clock phases at the pulse shaping circuits whose outputs are passed to the modulator drivers.

V. Conclusion

We have studied O-band DWDM analog coherent systems that use either discrete lasers or DR-EO frequency comb generators as Tx and LO light sources, evaluating the achieveable transmission distance in the presence of fiber Kerr nonlinearity, losses, noise and timing skew. The results indicate that O-band analog coherent systems are susceptible to degradation from fiber Kerr nonlinear effects.

Compared to systems using discrete lasers, comb-based systems are subject to about a 2-dB degradation of SNR because of losses from comb de-interleaving, flattening and demultiplexing, as well as noise from booster amplification. Nevertheless, when link losses are managed carefully, comb-based systems can support transmission distances required by all intra-data center links and some inter-data center links, even

with high-order modulation formats. For instance, 17-channel 16-QAM and 8-PSK comb systems can transmit over 10 km of fiber while maintaining a BER of 2.4×10^{-4} on all channels when additional link loss is kept below 2 dB and 7 dB, respectively. QPSK comb systems can support transmission distances exceeding 20 km with over 10 dB of loss margin.

We found that linear and nonlinear crosstalk causes the performance of both discrete-laser and comb-based systems to depend on timing skew between channels. For 16-QAM and 8-PSK systems, the peak-to-peak normalized skew ϵ should not exceed 0.1 and 0.2, respectively, in order to avoid reduction in achievable transmission distance. QPSK systems, however, are insensitive to timing skew impairments.

We have presented results for systems operating at a symbol rate of 56 Gbaud. Realizing systems using higher symbol rates, such as 100 Gbaud, requires careful design. Systems with higher symbol rates support lower achievable transmission distances and need wider channel spacing to avoid crosstalk.

Appendix A
Time Scales of Laser Phase Noise and Fiber Dispersion

In this section, we show that the coherence time of laser phase noise is much longer than the memory length of fiber chromatic dispersion. Hence, laser phase noise on the transmitted signal can be modeled as a constant phase offset when studying the effect of fiber propagation on system performance.

We define the coherence time of laser phase noise, τ_{pn}, as

$$\tau_{pn} = \frac{1}{2\pi\Delta\nu}, \tag{4}$$

where $\Delta\nu$ is the linewidth of the transmitter laser [32]. Assuming the transmitter laser linewidth is 1 MHz, the phase noise coherence time is $\tau_{pn} \approx 160$ ns. The phase noise coherence time becomes longer when using lasers with lower linewidth.

In the fiber, the longest relevant time scale associated with physical propagation is the dispersion-induced group delay spread between Ch. $p = 0$ and channel Ch. $p = p_0$. We thus define the memory length of fiber chromatic dispersion, τ_{cd}, as the group delay spread between Ch. 0 and Ch. p_0. Given O-band transmission ($D = 0$, $S \neq 0$), τ_{cd} is found by

$$\tau_{cd} = \frac{1}{2}|\beta_3|L\left(2\pi p_0 f_m\right)^2. \tag{5}$$

In Eq. (5), L is the fiber transmission length and f_m is the channel spacing. β_3 is related to the dispersion slope S by

$$\beta_3 = \left(\frac{\lambda^2}{2\pi c}\right)^2 S \tag{6}$$

where λ is the operating wavelength. We set the channel spacing to $f_m = 100$ GHz and use $S = 0.092$ ps/(nm$^2\cdot$ km) for O-band transmission. For $L = 80$ km on a 17-channel system ($p_0 = 8$), we find $\tau_{cd} \approx 77$ ps, indicating that the laser phase noise coherence time is much longer than the chromatic dispersion memory length. Shorter transmission distances results in shorter chromatic dispersion memory lengths. The phase noise therefore remains relatively constant over the memory length of chromatic dispersion effects.

Acknowledgment

The authors are grateful for helpful discussions with Nancy Yousry Ammar and Thomas Horton King. The authors would also like to thank Meta and the SystemX Alliance for supporting this work.

References

[1] A. A. M. Saleh, K. E. Schmidtke, R. J. Stone, J. F. Buckwalter, L. A. Coldren, and C. L. Schow, "INTREPID program: technology and architecture for next-generation, energy-efficient, hyper-scale data centers [Invited]," *J. Opt. Commun.*, vol. 13, no. 12, pp. 347–359, 2021.

[2] X. Zhou, R. Urata, and H. Liu, "Beyond 1 Tb/s intra-data center interconnect technology: IM-DD OR Coherent?" *J. Lightw. Technol.*, vol. 38, no. 2, pp. 475–484, 2020.

[3] E. Ip, A. P. T. Lau, D. J. F. Barros, and J. M. Kahn, "Coherent detection in optical fiber systems," *Opt. Express*, vol. 16, no. 2, pp. 753–791, 2008.

[4] A. Maharry, H. Andrade, S. Misak, J. Liu, Y. Xia, A. Wissing, G. Movaghar, V. Arrunategui-Norvick, E. D. Chansky, X. Du, A. A. M. Saleh, J. F. Buckwalter, L. Coldren, and C. L. Schow, "Integrated SOAs enable energy efficient intra-data center coherent links," *Opt. Express*, vol. 31, no. 11, pp. 17 480–17 493, 2023.

[5] J. K. Perin, A. Shastri, and J. M. Kahn, "Design of low-power DSP-Free coherent receivers for data center links," *J. Lightw. Technol.*, vol. 35, no. 21, pp. 4650–4662, 2017.

[6] A. Maharry, J. Liu, S. Misak, H. Andrade, L. A. Valenzuela, G. Gilardi, S. Liao, A. Liu, Y. Akulova, L. Coldren, J. F. Buckwalter, and C. L. Schow, "First demonstration of an O-Band coherent link for intra-data center applications," *J. Lightw. Technol.*, vol. 41, no. 21, pp. 6643–6650, 2023.

[7] R. W. Tkach, A. R. Chraplyvy, F. Forghieri, A. H. Gnauck, and R. M. Derosier, "Four-photon mixing and high-speed WDM systems," *J. Lightw. Technol.*, vol. 13, no. 5, pp. 841–849, 1995.

[8] X. Liu and Q. Fan, "Inter-Channel FWM mitigation techniques for 800G-LR4, 1.6T-LR8, 400G-ER4 and 5G fronthaul applications based on O-Band WDM," *J. Lightw. Technol.*, vol. 42, no. 3, pp. 1085–1094, 2024.

[9] J. G. Proakis and M. Salehi, *Digital Communications, 5th Edition*. New York: McGraw-Hill, 2008.

[10] Y. Miyamoto, A. Hirano, K. Yonenaga, A. Sano, H. Toba, K. Murata, and O. Mitomi, "320 Gbit/s (8 x 40 Gbit/s) WDM transmission over 367km with 120km repeater spacing using carrier-suppressed return-to-zero format," *Electron. Lett.*, vol. 35, no. 23, pp. 2041–2042, 1999.

[11] S. N. Shahi, S. Kumar, and X. Liang, "Analytical modeling of cross-phase modulation in coherent fiber-optic system," *Opt. Express*, vol. 22, no. 2, pp. 1426–1439, 2014.

[12] A. R. Chraplyvy, "Limitations on Lightwave Communications Imposed by Optical-Fiber Nonlinearities," *J. Lightw. Technol.*, vol. 8, no. 10, pp. 1548–1557, 1990.

[13] F. M. Madani and K. Kikuchi, "Design Theory of Long-Distance WDM Dispersion-Managed Transmission System," *J. Lightw. Technol.*, vol. 17, no. 8, pp. 1326–1335, 1999.

[14] M. Varani, G. Bellotti, A. Bononi, and C. Francia, "Analysis of cross-phase modulation induced intensity noise in high-speed dispersion compensated transmission systems," in *Proc. of LEOS 1998*, December 1998.

[15] G. Bellotti and S. Bigo, "Cross-Phase Modulation Suppressor for Multi-span Dispersion-Managed WDM Transmissions," *IEEE Photon. Technol. Lett.*, vol. 12, no. 6, pp. 726–728, 2000.

[16] A. Rizzo, A. Novick, V. Gopal, B. Y. Kim, X. Ji, S. Daudlin, Y. Okawachi, Q. Cheng, M. Lipson, A. L. Gaeta, and K. Bergman, "Massively scalable Kerr comb-driven silicon photonic link," *Nat. Photonics*, vol. 17, pp. 781–790, 2023.

[17] E. Berikaa, M. S. Alam, S. Bernal, R. Gutierrez-Castrejon, W. Li, Y. Hu, B. Krueger, F. Pittala, and D. V. Plant, "Next-Generation O-Band Coherent Transmission for 1.6 Tbps 10 km Intra-Datacenter Interconnects," *J. Lightw. Technol.*, vol. 42, no. 3, pp. 1126–1135, 2024.

[18] L. Lundberg, M. Mazur, A. Mirani, B. Foo, J. Schroder, V. Torres-Company, M. Karlsson, and P. A. Andrekson, "Phase-coherent lightwave communications with frequency combs," *Nat. Commun.*, vol. 11, no. 201, 2020.

[19] E. Chen, L. A. Coldren, and J. M. Kahn, "Design of Mode-Locked Semiconductor Laser Comb-Based Analog Coherent Links," *J. Lightw. Technol.*, vol. 41, no. 18, pp. 5930–5941, 2023.
[20] E. Temprana, E. Myslivet, L. Liu, V. Ataie, A. Wiberg, B. P. P. Kuo, N. Alic, and S. Radic, "Two-fold transmission reach enhancement enabled by transmitter-side digital backpropagation and optical frequency comb-derived information carriers," *Opt. Express*, vol. 23, no. 16, pp. 20 774–20 783, 2015.
[21] N. Alic, E. Myslivets, E. Temprana, B. P. P. Kuo, and S. Radic, "Nonlinearity Cancellation in Fiber Optic Links Based on Frequency Referenced Carriers," *J. Lightw. Technol.*, vol. 32, no. 15, pp. 2690–2698, 2014.
[22] S. Bernal, M. Dumont, E. Berikaa, C. St-Arnault, Y. Hu, R. G. Castrejon, Z. Wei, A. D'Errico, A. Bigongiari, L. Giorgi, S. Stracca, R. Brunner, S. Lessard, F. Cavaliere, J. Bowers, and D. V. Plant, "8.5 Tbps Net SiP O-band Coherent Transmission over 10 km Using a Quantum-Dot Mode-Locked Comb Laser," in *Proc. of OFC 2024*, March 2024.
[23] T. Hirokawa, S. Pinna, N. Hosseinzadeh, A. Maharry, H. Andrade, J. Liu, T. Meissner, S. Misak, G. Movaghar, L. A. Valenzuela, Y. Xia, S. Bhat, F. Gambini, J. Klamkin, A. A. M. Saleh, L. Coldren, J. F. Buckwalter, and C. L. Schow, "Analog Coherent Detection for Energy Efficient Intra-Data Center Links at 200 Gbps Per Wavelength," *J. Lightw. Technol.*, vol. 39, no. 2, pp. 520–531, 2021.
[24] E. Chen, B. Buscaino, and J. M. Kahn, "Phase Noise Analysis of Resonator-Enhanced Electro-Optic Comb-Based Analog Coherent Receivers," *J. Lightw. Technol.*, vol. 40, no. 21, pp. 7117–7128, 2022.
[25] Y. Hu, M. Yu, B. Buscaino, N. Sinclair, D. Zhu, R. Cheng, A. Shams-Ansari, L. Shao, M. Zhang, J. M. Kahn, and M. Loncar, "High-efficiency and broadband on-chip electro-optic frequency comb generators," *Nat. Photonics*, vol. 16, pp. 679–685, 2022.
[26] B. Buscaino, M. Zhang, and M. L. an Joseph M. Kahn, "Design of Efficient Resonator-Enhanced Electro-Optic Frequency Comb Generators," *J. Lightw. Technol.*, vol. 38, no. 6, pp. 1400–1413, 2020.
[27] C. H. Henry, "Theory of the Phase Noise and Power Spectrum of a Single Mode Injection Laser," *IEEE J. Quantum Electron.*, vol. QE-19, no. 9, pp. 1391–1397, 1983.
[28] L. Chang, S. Liu, and J. E. Bowers, "Integrated optical frequency comb technologies," *Nat. Photonics*, vol. 16, pp. 95–108, 2022.
[29] E. Ip and J. M. Kahn, "Compensation of Dispersion and Nonlinear Impairments Using Digital Backpropagation," *J. Lightw. Technol.*, vol. 26, no. 20, pp. 3416–3425, 2008.
[30] U. of Maryland Photonics Research Laboratory, "SSPROP," https://photonics.umd.edu/software/ssprop/.
[31] J. K. Perin, A. Shastri, and J. M. Kahn, "Coherent Data Center Links," *J. Lightw. Technol.*, vol. 39, no. 3, pp. 730–741, 2021.
[32] G. P. Agrawal, *Fiber-Optic Communication Systems*, 3rd ed. Wiley & Sons, 2002.
[33] P. Anslow, "RS(544,514) FEC performance," 2016, online; accessed 11 May 2024.
[34] B. Buscaino, E. Chen, J. W. Stewart, T. Pham, and J. M. Kahn, "External vs. Integrated Light Sources for Intra-Data Center Co-Packaged Optical Interfaces," *J. Lightw. Technol.*, vol. 39, no. 7, pp. 1984–1996, 2021.
[35] J. K. Perin, A. Shastri, and J. M. Kahn, "Data center links beyond 100 Gbit/s per wavelength," *Opt. Fiber Technol.*, vol. 44, pp. 69–85, 2018.

Elizabeth Chen (Student Member, IEEE) received the B.A.Sc. degree in Engineering Science from the University of Toronto, Toronto, ON, Canada, in 2019, and the M.S. degree in Electrical Engineering from Stanford University Stanford, CA, USA, in 2021. She is working towards her Ph.D. degree in Electrical Engineering at Stanford University. Her current research interests include optical communications, optical frequency combs, and coherent data center links.

Joseph M. Kahn (Fellow, IEEE) received A.B., M.A. and Ph.D. degrees in Physics from the University of California, Berkeley in 1981, 1983 and 1986. In 1987-1990, Kahn was at AT&T Bell Laboratories. In 1989, he demonstrated the first successful synchronous (i.e., coherent) detection using semiconductor lasers, achieving record receiver sensitivity. In 1990-2003, Kahn was on the Electrical Engineering and Computer Sciences faculty at Berkeley. He demonstrated coherent detection of QPSK in 1992. In 1999, D.-S. Shiu and Kahn published the first work on probabilistic shaping for optical communications. In the 1990s and early 2000s, Kahn and collaborators performed seminal work on indoor and outdoor free-space optical communications and multi-input multi-output wireless communications. In 2000, Kahn and K.-P. Ho founded StrataLight Communications, whose 40 Gb/s-per-wavelength long-haul fiber transmission systems were deployed widely by AT&T, Deutsche Telekom, and other carriers. In 2002, Ho and Kahn applied to patent the first electronic compensation of fiber Kerr nonlinearity. StrataLight was acquired by Opnext in 2009. In 2003, Kahn became a Professor of Electrical Engineering in the E. L. Ginzton Laboratory at Stanford University. Kahn and collaborators have extensively studied rate-adaptive coding and modulation, as well as digital signal processing for mitigating linear and nonlinear impairments in coherent systems. In 2008, E. Ip and Kahn (and G. Li independently) invented simplified digital backpropagation for compensating fiber Kerr nonlinearity and dispersion. Since 2004, Kahn and collaborators have studied propagation, modal statistics, spatial multiplexing and imaging in multi-mode fibers, elucidating principal modes and demonstrating transmission beyond the traditional bandwidth-distance limit in 2005, deriving the statistics of coupled modal group delays and gains in 2011, and deriving resolution limits for imaging in 2013. Kahn's current research addresses optical frequency comb generators, coherent data center links, rate-adaptive access networks, fiber Kerr nonlinearity mitigation, ultra-long-haul submarine links, and optimal free-space transmission through atmospheric turbulence. Kahn received the National Science Foundation Presidential Young Investigator Award in 1991. In 2000, he became a Fellow of the IEEE.